

---

# Posterolateral Defect of the Normal Human Heart Investigated with Nitrogen-13-Ammonia and Dynamic PET

Richard M. de Jong, Paul K. Blanksma, Antoon T.M. Willemsen, Rutger L. Anthonio, Joan G. Meeder, Jan Pruim, Wim Vaalburg and Kong I. Lie

*Department of Cardiology and National Research PET Center, University Hospital Groningen, The Netherlands*

---

The posterolateral defect is a common artifact seen when static  $^{13}\text{N}$ -ammonia imaging with PET is used to assess myocardial perfusion. The aim of this study was to compare dynamic and static  $^{13}\text{N}$ -ammonia PET and to obtain more insight into the cause of the posterolateral defect. **Methods:** Dynamic  $^{13}\text{N}$ -ammonia PET was performed in 19 healthy nonsmoking volunteers at rest. Perfusion was assessed in the early phase of the study using a curve fit method over the first 90 sec. Nitrogen-13 accumulation (static PET) was assessed 4 to 8 min after injection. Each study was normalized to a mean of 100. The average distribution of normalized perfusion and activity was calculated in 24 segments. Heterogeneity of both activity and perfusion distribution were assessed and the activity distribution was compared with perfusion distribution. **Results:** Perfusion distribution was homogeneous, with the exception of the inferior and apical regions. Activity distribution was inhomogeneous, with a lower activity in the posterolateral and apical regions. In the whole left ventricle, significant differences in distribution were found between static and dynamic imaging. **Conclusion:** Perfusion distribution was significantly different on dynamic images compared to static images. The posterolateral defect was not found on dynamic images. The posterolateral defect and other inhomogeneities in activity distribution are caused by tracer-dependent features, probably a redistribution of metabolites of  $^{13}\text{N}$ -ammonia.

**Key Words:** myocardial perfusion; nitrogen-13-ammonia; posterolateral defect; parametric polar map; positron emission tomography

**J Nucl Med 1995; 36:581-585**

---

**P**ET has proven to be an accurate technique for studying myocardial perfusion (1). Although dynamic PET studies give the opportunity to obtain quantitative information about myocardial perfusion (ml/min/g tissue), many PET centers use static PET imaging only. Several positron-emitting trac-

ers have been used to study myocardial perfusion [e.g.,  $^{82}\text{Rb}$  (2),  $^{13}\text{N}$ -ammonia (3,4) and  $^{15}\text{O}$ -water (5)].

By using  $^{13}\text{N}$ -ammonia as a perfusion tracer and static PET imaging, several groups have found inhomogeneities in  $^{13}\text{N}$  activity distribution in the left ventricular myocardium of normal subjects (6-11). Diminished activity in the posterolateral area, the posterolateral defect, has often been reported and hampers the interpretation of static PET images of patients with coronary artery disease of the circumflex artery. Some investigators have used dynamic  $^{13}\text{N}$  PET imaging to confirm the presence of diminished perfusion in the posterolateral region (9,10). Others, however, have reported homogeneous distribution of activity and perfusion (12-16). Dynamic perfusion studies using  $^{15}\text{O}$ -water (17-20) and static PET studies with  $^{82}\text{Rb}$  (21) did not show diminished perfusion in the posterolateral area. This study compares the results of static and dynamic  $^{13}\text{N}$ -ammonia PET data analyses to obtain more insight in the cause of the posterolateral defect. Therefore, the distribution of  $^{13}\text{N}$  activity, as found during static imaging, was compared with the distribution of myocardial perfusion in the whole left ventricle of healthy volunteers using dynamic  $^{13}\text{N}$ -ammonia PET.

## METHODS

### Population

Nineteen healthy, nonsmoking volunteers (5 female, 14 male), age  $35.3 \pm 11.7$  yr, were studied with  $^{13}\text{N}$ -ammonia in a resting condition. No subject ever had symptoms suggestive of coronary artery disease. All subjects had a normal ECG and none of them used medication. Smoking volunteers were explicitly excluded because such volunteers show abnormalities in myocardial perfusion, as proven in separate studies from our institute (22). The study protocol was approved by the hospital's Medical Ethics Committee and volunteers gave written informed consent.

### PET

All volunteers were instructed to refrain from caffeinated beverages in the 24 hr prior to testing. Volunteers were positioned in a 951 Siemens ECAT positron camera. This camera images 31 planes simultaneously over a length of 10.8 cm. Measured resolution of the system is 6 mm FWHM. Data were automatically corrected for accidental coincidence and deadtime. Volunteers were positioned with a rectilinear scan. Thereafter, transmission

---

Received Mar. 31, 1994; revision accepted Aug. 8, 1994.

For correspondence or reprints contact: Paul K. Blanksma, MD, Dept. of Cardiology, University Hospital Groningen, Oostersingel 59, 9700 RB Groningen, The Netherlands.

scanning with a  $^{68}\text{Ge}/^{68}\text{Ga}$  retractable ring source was performed for 20 min to correct for photon attenuation. The transmission scan was followed by a  $^{13}\text{N}$ -ammonia emission scan, starting with a rapid bolus injection of 370 MBq  $^{13}\text{N}$ -ammonia. Dynamic imaging continued for 8 min using a protocol of 14 frames:  $12 \times 10$  sec,  $1 \times 2$  min and  $1 \times 4$  min.

### Data Analysis

PET data were analyzed using standard ECAT software plus additional applications written at our institution. Distribution was assessed using semiquantitative ( $^{13}\text{N}$  activity) and parametric (quantified perfusion) polar map display. The 31 contiguous transaxial images were reorientated into ten left ventricular short-axis slices. In the last frame, a mid left ventricular transaxial plane was selected for interactive definition of the long-axis as well as the lateral and septal borders of the left ventricle. A second image plane perpendicular to the initial transaxial plane was displayed and the long-axis was interactively defined for reorientation to short-axis images consisting of ten planes from apex to base. In each plane of the short-axis images, inner and outer contours of the left ventricle were defined with two circles. Subsequently, the myocardium in the ten different short-axis slices was divided into 48 segments of 7.5 degrees each. Thus, the total heart was divided in 480 segments. Using the maximum activity, time-activity curves were assessed in each segment of each slice. Blood pool was defined in three slices near the base and the average was used to obtain a single arterial tracer input curve (23). In the 480 segments, absolute myocardial perfusion was determined by the model described by Bellina et al. (24), which uses a curve fit method over the first 90 sec. A correction for perfusion-mediated extraction of the tracer was applied as used by Schelbert et al. (3):

$$E = E_0 \cdot (1 - 0.607e^{-1.25/\text{Flow}}).$$

For the static studies, data of the last frame (4 to 8 min) were used and the maximum activity in each segment was applied. Because this study was intended to investigate distribution of perfusion and radioactivity solely, each individual  $^{13}\text{N}$ -ammonia study (both static and dynamic) was normalized to a mean of 100; in each individual study, each segment was divided by the mean of the 480 segments of that study and multiplied by 100. Average perfusion distribution was assessed by dividing the sum of the normalized perfusion studies by the total of studies, and average distribution of activity was assessed by dividing the sum of the normalized activity studies by the total of studies. The advantage of a normalization to the mean is that every  $^{13}\text{N}$ -ammonia study contributes the same weight to the final outcome of the average distribution of the group. Finally, the left ventricle was divided in 24 regions, three rings consisting of eight regions each, in which normalized perfusion and activity were determined for statistical analysis (Fig. 1).

### Statistical Analysis

The results are presented as means  $\pm$  s.d. To assess homogeneity in distribution, an ANOVA test with multiple comparison and Bonferroni correction was used in both the static and the dynamic groups. To test differences in global distribution between  $^{13}\text{N}$  activity and myocardial perfusion, MANOVA was performed. If a significant difference was found, a paired Student's t-test was used for statistical analysis of regional differences between distribution of  $^{13}\text{N}$  activity and myocardial perfusion in the 24 regions. A p value of  $<0.05$  was considered significantly different.

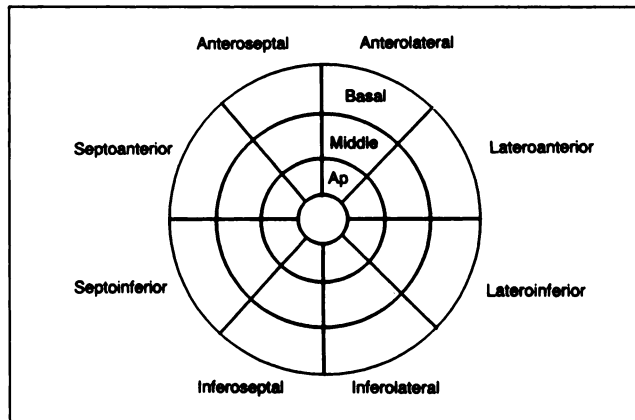


FIGURE 1. Polar map representing the 24 regions in which activity and perfusion are determined.

## RESULTS

### Dynamic Imaging

Mean myocardial perfusion was  $95.8 \pm 18.6$  ml/min/100 g tissue (Fig. 2B). By applying ANOVA, a group of 18 regions was found which were not significantly different when compared to each other. The six other regions consisted of four regions in the apical zone which were lower and two regions in the inferior zone which were higher (Table 1). Hence, the distribution of myocardial perfusion, as assessed with the ANOVA test, is homogeneous with the exception of the inferior and apical region.

### Static Imaging

The largest group of regions not significantly different in comparison consisted of ten regions (Fig. 2A). All other regions were significantly different compared to this group (Table 1). Thus, the distribution of  $^{13}\text{N}$  activity is inhomogeneous. The lowest activity was found in the lateral and posterolateral area, the highest in the anteroseptal and inferior areas.

### Dynamic Versus Static PET

With MANOVA, significant differences in global distribution were found between static and dynamic  $^{13}\text{N}$ -ammonia PET. When comparing the normalized radioactivity (static images) in the different regions with the normalized perfusion values (dynamic images) with a paired Student's t-test, significant differences ( $p < 0.05$ ) were found among 14 regions (Table 1). The relative homogeneous distribution of myocardial perfusion implies a relative homogeneous distribution of activity at 90 sec. By dividing the static image by the dynamic image, a redistribution image of  $^{13}\text{N}$  activity between 90 sec and 4 to 8 min after injection was obtained (Fig. 2C).

## DISCUSSION

In this study, 90-sec dynamic  $^{13}\text{N}$ -ammonia PET perfusion images are compared with the activity distribution in a static image obtained with the same tracer 4–8 min after injection. A statistically significant difference was found between the distribution of myocardial perfusion obtained by dynamic

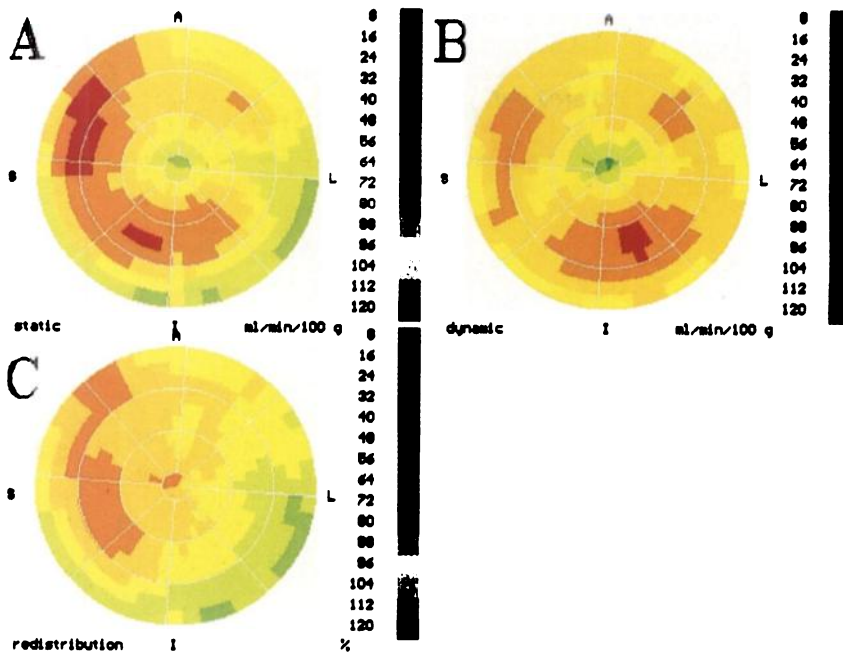


**FIGURE 2.** (A) Average distribution of normalized  $^{13}\text{N}$  activity in static images obtained from 4 to 8 min after tracer injection. Relatively lower activity in the lateral regions can be seen. (B) Average distribution of normalized myocardial perfusion in the dynamic images derived from data obtained 0 to 90 sec after tracer injection. Higher perfusion is found in the inferior region and lower perfusion in the anteroapical region due to spillover and partial volume effects. (C) Ratio of B over A. Redistribution can be noticed from the posterolateral to the septal regions.

analysis and the activity distribution in the static image. The static images showed lower activity in the posterolateral portion of the left ventricle and an overall inhomogeneous distribution of  $^{13}\text{N}$  activity accumulation. Dynamic  $^{13}\text{N}$ -ammonia PET showed more homogeneous perfusion. Experimental data on the subject of spatial distribution indicate that perfusion in mammalian hearts is heterogeneous (25,26), although specific regions of hypo- or hyperperfusion have not been mentioned. In these studies, the coefficient of variation (or relative dispersion =  $\text{s.d./mean}$ ) was used as a measure of heterogeneity which has the disadvantage of being influenced by the size of myocardial samples employed to analyze perfusion. Fractional analysis is one technique that may solve these problems (27), but the obtained parameters only give information about global heterogeneity and not an indication of specific regions that have higher or lower perfusion or radioactivity.

Inhomogeneous  $^{13}\text{N}$  activity in the left ventricular myocardium, particularly diminished activity in the posterolateral part of the left ventricle, has been previously reported. However, homogeneous distribution of activity also has been reported. Most of these groups did not primarily focus on the distribution of activity or perfusion which may influence their results and statements on heterogeneity. The contradictions in the literature about homogeneity of radioactivity distribution in the normal human heart can probably be explained by differences in equipment and study design, e.g., camera, number and selection of normal subjects, number and volume of regions investigated and kind of normalization procedure used. Most of these studies used older PET cameras that have a limited number of detector rings and lower resolution, and radioactivity was only measured in a few transaxial slices. Furthermore, criteria for heterogeneity are often not clear and statements

about it are based on different analyses, e.g., visual (13,14), circumferential profile analysis (14) and different statistical parameters and tests.

Several hypotheses have been formulated on the cause of the posterolateral defect and other inhomogeneities in  $^{13}\text{N}$  activity in the left ventricular myocardium. Factors that could explain these inhomogeneities are absolute myocardial perfusion inhomogeneity and technical and tracer-dependent features.

#### Absolute Myocardial Perfusion Inhomogeneity

No firm evidence is available to support physiologically lower perfusion of the posterolateral wall of the left ventricle. In most studies using dynamic PET to assess myocardial perfusion, diminished perfusion of the posterolateral part of the left ventricle has not been observed (15–20). Moreover, dynamic  $^{13}\text{N}$ -ammonia PET did not show diminished perfusion in this area. Thus, myocardial perfusion inhomogeneity can be excluded as an explanation for the posterolateral defect.

#### Technical Features

Technical features which may influence the results of  $^{13}\text{N}$ -ammonia studies are: ungated data acquisition causing blurring of the myocardial wall, partial volume effect, spillover effect, limited scatter correction and effects of reorientation of transaxial slices to short-axis slices (28). The lower perfusion and activity in the apical part of the myocardium can be explained by a partial volume effect. The higher perfusion and radioactivity encountered in the inferior region is probably an artifact caused by spillover from the liver. It seems unlikely that technical factors were responsible for the reduction of  $^{13}\text{N}$  activity seen in the posterolateral wall, because this reduction has not been

**TABLE 1**  
Distribution of <sup>13</sup>N activity and Perfusion (Normalized Values)

Region	Dynamic PET			Static PET			p
	Mean	s.d.	ANOVA	Mean	s.d.	ANOVA	
<b>Basal Ring</b>							
Inferolateral	102.4	8.2		91.3	6.9	*	§
Lateroinferior	103.0	7.0		88.3	6.6	*	§
Lateroanterior	99.0	6.1		93.3	5.2	*	‡
Anterolateral	100.0	9.5		99.5	6.6		
Anteroseptal	100.7	10.7		107.7	7.4	*	†
Septoanterior	105.1	9.0		113.3	7.9	*	‡
Septoinferior	102.4	9.1		101.5	6.2		
Inferoseptal	101.3	10.9		94.1	8.1		‡
<b>Middle Ring</b>							
Inferolateral	114.2	12.3	*	111.0	8.6	*	
Lateroinferior	108.3	7.6		98.5	6.4		§
Lateroanterior	102.7	6.8		95.0	5.9		‡
Anterolateral	107.0	5.9		106.1	5.4	*	
Anteroseptal	99.6	4.6		104.5	4.6	*	‡
Septoanterior	105.1	5.4		114.6	4.1	*	§
Septoinferior	103.2	6.4		112.0	4.5	*	§
Inferoseptal	110.7	6.2	*	115.3	7.0	*	†
<b>Apical Ring</b>							
Inferolateral	105.9	11.1		104.6	8.3	*	
Lateroinferior	101.5	11.2		99.4	6.4		
Lateroanterior	92.1	6.7	*	91.5	5.7	*	
Anterolateral	92.3	6.1	*	94.0	4.3		
Anteroseptal	92.9	5.4	*	96.5	4.1		†
Septoanterior	92.3	6.3	*	98.0	4.4		‡
Septoinferior	98.1	7.6		100.7	7.0		
Inferoseptal	103.5	7.6		105.3	6.7	*	

\*Region significantly different in comparison to the homogeneous group, meaning the largest group of regions not significantly different compared to each other ( $p < 0.05$ ). † $<0.05$ ; ‡ $<0.005$ ; § $<0.0005$ . Significant differences between dynamic and static normalized values are based on paired Student's t-test.

described with other perfusion tracers nor was measured in this study by dynamic <sup>13</sup>N-ammonia PET. A relatively homogeneous perfusion was found. Furthermore, previous research excluded possible artifacts due to wall motion or partial volume effect (11). Thus, technical features can be excluded as an explanation for the posterolateral defect.

#### Tracer-Dependent Features

A real regional variation in the normal myocardial distribution of <sup>13</sup>N-ammonia and the metabolites formed in the myocytes may be possible. An explanation may be regional differences in enzyme concentrations or enzyme activity, as proposed by Laubenbacher et al. (7). The trapping of <sup>13</sup>N in the myocardium involves at least one enzymatic reaction (29), in which glutamine synthetase is the most important enzyme (3,30). Further studies of the concentration and activity distribution of this enzyme are needed to elucidate the cause of the posterolateral defect. Regional differences in <sup>13</sup>N-ammonia metabolism could be linked to an overall metabolic heterogeneity in the human heart as shown in previous studies with regard to the distribution of <sup>18</sup>F-fluorodeoxyglucose (19,31).

Another possible explanation for the posterolateral de-

fect is an inhomogeneous release and/or uptake of metabolites of <sup>13</sup>N-ammonia. Further investigation of the behavior of <sup>13</sup>N-ammonia metabolites is needed to test this hypothesis. Nitrogen-13-ammonia is the main component of blood radioactivity during the first 2 min after injection. The relative contribution of ammonia to total blood radioactivity, however, declines rapidly (32). This could have an important impact on static <sup>13</sup>N-ammonia PET imaging. Data used for static imaging are obtained from 4 min after injection and could be affected by metabolites of ammonia, whereas data applied for assessing perfusion in dynamic <sup>13</sup>N-ammonia PET are obtained in the first 90 sec of imaging and will probably be less affected by metabolites. Static imaging during the first minutes gives an image with little contrast between radioactivity in the blood in the ventricle and radioactivity in the myocardial tissue and therefore cannot be used to assess myocardial perfusion.

#### CONCLUSION

This study demonstrates a clear and statistically significant difference between <sup>13</sup>N activity distribution and perfusion distribution as determined by dynamic <sup>13</sup>N-ammonia PET

imaging. These differences in distribution are not only present in the posterolateral region but are observed in the whole left ventricular myocardium. The posterolateral defect and other inhomogeneities in static  $^{13}\text{N}$ -ammonia PET images can be explained by tracer-dependent features. Although this study did not directly measure the behavior of  $^{13}\text{N}$ -ammonia metabolites, it seems likely that there is redistribution of these metabolites between 90 sec and 4 to 8 min after injection. Dynamic  $^{13}\text{N}$ -ammonia PET has major advantages compared to static  $^{13}\text{N}$ -ammonia PET imaging. It gives a more homogeneous distribution in the normal human heart and generates absolute figures about myocardial perfusion. Particularly, interpretation of the myocardial region perfused by the circumflex artery will give less problems with dynamic  $^{13}\text{N}$ -ammonia PET compared to static  $^{13}\text{N}$ -ammonia PET imaging. Moreover, quantitative measurement of myocardial perfusion can address issues such as absolute perfusion reserve or the appropriateness of a given level of perfusion to a particular set of physiological conditions and thus is advantageous for the study of the myocardium as a whole (33). Investigation of the behavior of  $^{13}\text{N}$ -ammonia metabolites and distribution of glutamine synthetase in the myocardium is needed to further elucidate the cause of the posterolateral defect.

## REFERENCES

1. Wisenberg G, Schelbert HR, Hoffman EJ, et al. In vivo quantitation of regional myocardial blood flow by positron emission computed tomography. *Circulation* 1981;63:1248-1258.
2. Selwyn AP, Allan RM, L'Abbate A, et al. Relation between regional myocardial uptake of rubidium-82 and perfusion: absolute reduction of cation uptake in ischemia. *Am J Cardiol* 1982;50:112-121.
3. Schelbert HR, Phelps ME, Huang SC, et al. N-13 ammonia as an indicator of myocardial blood flow. *Circulation* 1981;63:1259-1272.
4. Shah A, Schelbert HR, Schwaiger M, et al. Measurement of regional myocardial blood flow with N-13 ammonia and PET in intact dogs. *J Am Coll Cardiol* 1985;5:92-100.
5. Bergmann SR, Fox KA, Rand AL, et al. Quantification of regional myocardial blood flow in vivo with  $\text{H}_2^{15}\text{O}$ . *Circulation* 1984;70:724-733.
6. Berry JJ, Baker JA, Pieper KS, Hanson MW, Hoffman JM, Coleman RE. The effect of metabolic milieu on cardiac PET imaging using fluorine-18-deoxyglucose and nitrogen-13-ammonia in normal volunteers. *J Nucl Med* 1991;32:1518-1525.
7. Laubenbacher C, Rothley J, Sitomer J, et al. An automated analysis program for the evaluation of cardiac PET studies: initial results in the detection and localization of coronary artery disease using nitrogen-13-ammonia. *J Nucl Med* 1993;34:968-978.
8. Porenta G, Kuhle W, Czernin J, et al. Semiquantitative assessment of myocardial blood flow and viability using polar map displays of cardiac PET images. *J Nucl Med* 1992;33:1628-1636.
9. Krivokapich J, Smith GT, Huang SC, et al. Nitrogen-13 ammonia myocardial imaging at rest and with exercise in normal volunteers. Quantification of absolute myocardial perfusion with dynamic PET. *Circulation* 1989;80:1328-1337.
10. Baudhuin T, Melin J, Marwick T, et al. Regional uptake and blood flow variations with N-13 ammonia in normal subjects do not correlate with flow or metabolic measurements by other methods [Abstract]. *J Nucl Med* 1992;33:837.
11. Porenta G, Czernin J, Huang SC, Kuhle W, Brunken RC, Schelbert HR. Dynamic and gated PET N-13 ammonia imaging confirms inhomogeneous perfusion in normal subjects [Abstract]. *J Nucl Med* 1993;34:35P.
12. Schelbert HR, Wisenberg G, Phelps ME, et al. Noninvasive assessment of coronary stenoses by myocardial imaging during pharmacologic coronary vasodilatation. VI. Detection of coronary artery disease in human beings with intravenous N-13 ammonia and positron computed tomography. *Am J Cardiol* 1982;49:1197-1207.
13. Tamaki N, Yonekura Y, Senda M, et al. Myocardial positron computed tomography with  $^{13}\text{N}$ -ammonia at rest and during exercise. *Eur J Nucl Med* 1985;11:246-251.
14. Yonekura Y, Tamaki N, Senda M, et al. Detection of coronary artery disease with  $^{13}\text{N}$  ammonia and high-resolution positron emission computed tomography. *Am Heart J* 1987;113:645-654.
15. Hutchins GD, Schwaiger M, Rosenspire KC, Krivokapich J, Schelbert H, Kuhl DE. Noninvasive quantification of regional blood flow in the human heart using N-13 ammonia and dynamic PET imaging. *J Am Coll Cardiol* 1990;15:1032-1042.
16. Czernin J, Müller P, Chan S, et al. Influence of age and hemodynamics on myocardial blood flow and flow reserve. *Circulation* 1993;88:62-69.
17. Bergmann SR, Herrero P, Markham J, Weinheimer CJ, Walsh MN. Non-invasive quantitation of myocardial blood flow in human subjects with oxygen-15-labeled water and positron emission tomography. *J Am Coll Cardiol* 1989;14:639-652.
18. Iida H, Kanno I, Takahashi A, et al. Measurement of absolute myocardial blood flow with  $\text{H}_2^{15}\text{O}$  and dynamic PET. Strategy for quantification in relation to the partial-volume effect. *Circulation* 1988;78:104-115.
19. Gropler RJ, Siegel BA, Lee KJ, et al. Nonuniformity in myocardial accumulation of fluorine-18-fluorodeoxyglucose in normal fasted humans. *J Nucl Med* 1990;31:1749-1756.
20. Senneff MJ, Geltman EM, Bergmann SR, Hartman J. Noninvasive delineation of the effects of moderate aging on myocardial perfusion. *J Nucl Med* 1991;32:2037-2042.
21. Sitomer J, Yang SH, Wolfe ER, Hutchins G, Schwaiger M. Automated three dimensional analysis of static cardiac PET studies [Abstract]. *J Nucl Med* 1992;33:1008.
22. Meeder JG, Blanksma PK, Anthonio RL, et al. Myocardial perfusion and hemodynamics in healthy smoking volunteers: evidence for autonomic and endothelial dysfunction [Abstract]. *J Nucl Med* 1994;35:3P.
23. Weinberg IN, Huang SC, Hoffman EJ, et al. Validation of PET acquired input functions for cardiac studies. *J Nucl Med* 1988;29:241-247.
24. Bellina CR, Parodi O, Camici P, et al. Simultaneous in vitro and in vivo validation of nitrogen-13 ammonia for the assessment of regional myocardial blood flow. *J Nucl Med* 1990;31:1335-1343.
25. Marcus ML, Kerber RE, Erhardt JC, Falsetti HL, Davis DM, Abboud FM. Spatial and temporal heterogeneity of left ventricular perfusion in awake dogs. *Am Heart J* 1977;94:748-754.
26. Franzen D, Conway RS, Zhang H, Sonnenblick EH, Eng C. Spatial heterogeneity of local blood flow and metabolic content in dog hearts. *Am J Physiol* 1988;254:344-353.
27. Bassingthwaite JB, King RB, Roger SA. Fractal nature of regional myocardial blood flow heterogeneity. *Circ Res* 1989;65:578-590.
28. Kuhle WG, Porenta G, Huang SC, Phelps ME, Schelbert HR. Issues in the quantitation of reoriented cardiac PET images. *J Nucl Med* 1992;33:1235-1242.
29. Krivokapich J, Huang SC, Phelps ME, MacDonald NS, Shine KI. Dependence of  $^{13}\text{N}$ -ammonia myocardial extraction and clearance on flow and metabolism. *Am J Physiol (Heart Circ Physiol)* 1982;242:H536-H542.
30. Bergmann SR, Hack S, Tewson T, Welch MJ, Sobel BE. The dependence of accumulation of  $^{13}\text{N}$ -ammonia by myocardium on metabolic factors and its implications for quantitative assessment of perfusion. *Circulation* 1980;61:34-43.
31. Hicks R, Herman W, Kalf V, et al. Quantitative evaluation of regional substrate metabolism in the human heart by positron emission tomography. *J Am Coll Cardiol* 1991;18:101-111.
32. Rosenspire KC, Schwaiger M, Mangner TJ, Hutchins GD, Sutorik A, Kuhl DE. Metabolic fate of [ $^{13}\text{N}$ ]ammonia in human and canine blood. *J Nucl Med* 1990;31:163-167.
33. Gerwitz H. Parametric images for quantitative measurements of regional myocardial blood flow in humans: a step in the right direction. *J Nucl Med* 1993;34:862-864.